FOA 4 RAPPORT
C 4346-23
Mars 1968

COMPRESSED ATOMS
II. APPLICATION TO Al AND Fe

K-F Berggren A Fröman

This report is issued by
The Research Institute of National Defence,
Stockholm 80, Sweden
FÖRSVARETS FORSKNINGSANSTALT
AVDELNING 4
Stockholm

FOA RAPPORTKATEGORIER

Rapporter avsedda för spridning utanför FOA utges i följande kategorier:

FOA A-rapport. Innehåller huvudsakligen för totalförsvaret avsedd och tillrättalagd redovisning av ett, som regel avslutat, arbete. Förekommer som öppen (A-) och hemlig (AH-) rapport.

FOA B-rapport. Innehåller för vidare spridning avsedd redovisning av öppet vetenskapligt eller tekniskt-vetenskapligt originalarbete av allmänt intresse. Utges i FOA skriftserie "FOA Reports" eller publiceras i FOA utomstående tidskrift, i vilket senare fall särtryck distribueras av FOA under beteckningen "FOA Reprints".

FOA C-rapport. Innehåller för spridning inom och utom FOA (i vissa fall enbart inom FOA) avsedd redovisning av arbete, t ex i form av delrapport, preliminärrapport eller metodikrapport. Förekommer som öppen (C-) och hemlig (CH-) rapport.

FOA-RAPPORTS STATUS

FOA-rapports status är att författaren (författarna) svarar för rapportens innehåll, t ex för att angivna resultat är riktiga, för gjorda slutsatser och rekommendationer etc.

FOA svarar - genom att rapporten godkänts för utgivning som FOA-rapport - för att det redovisade arbetet utförts i överensstämmelse med "vetenskap och praxis" på ifrågavarande område.

I förekommande fall tar FOA ställning till i rapporten gjorda bedömningar etc - detta anges i så fall i särskild ordning, t ex i missiv.

FOA-RAPPORTS REGISTRERING

Fr o m den 1. 7. 1966 registreras FOA-rapport enligt följande exempel:

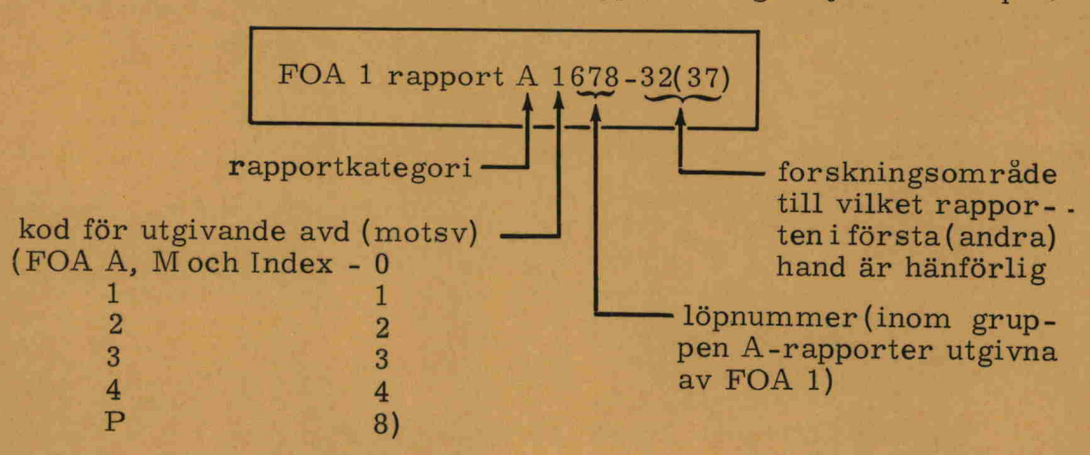

Försvarets forskningsanstalt
Avdelning 4
Stockholm 80

FOA 4 rapport
C 4346-23
Mars 1968

COMPRESSED ATOMS.
II. APPLICATION TO Al AND Fe

by K-F Berggren and A Fröman

Antal blad 36

Abstract

The spherical cellular model, which treats an atom confined to a finite spherical volume, is used to make a quantum-mechanical study of some properties of Al and Fe at various compressions. The calculations are performed with a Thomas-Fermi potential and an approximate self-consistent potential in the Hartree-Fock--Slater equations. The pressure-density relation at 0° K and some electronic properties such as bandstructure and specific heat are calculated and compared with results of experiment and other theories. It appears that the spherical cellular model in its present version does not give reliable quantitative results but qualitatively it gives an improvement on the statistical models.

Sammanfattning

Den sfäriska cellular modellen, som beskriver en atom innesluten i en ändlig sfärisk volym, används för att kvantmekaniskt studera några egenskaper hos Al och Fe vid olika kompressioner. Beräkningar har utförts med en Thomas-Fermi potential och en approximativ självkonsistent potential i Hartree-Fock-Slater ekvationerna. Tryck-tätthetssamband vid 0° K och några elektroniska egenskaper såsom bandstruktur och specifik värme har beräknats och jämförts med experimentella och andra teoretiska resultat. Det visar sig att den sfäriska cellular modellen i dess nuvarande form inte ger tillförlitliga kvantitativa resultat men kvalitativt utgör den en förbättring av de statiska modellerna.

FOA uppdrag nr: 2322

Rapporten utsänd till:
AB Atomenergi (2 ex), Inst f teor fysik Uppsala, Lund, Inst f matematik KTH, FOA M, FOA 1, FOA 2 (3 ex), FOA 3 (2 ex)
FOA 4: 20, 40, 50, 60, 61 (70 ex), 62, 71, 80, 90

Contents.

1. Introduction.

In a previous report[1] simplified electronbands and the zeroisotherm were calculated for Al by means of a spherical cellular method, the details of which are described in the same report and by Brooks[2] and Gandel'man[3]. With the model potential chosen, a Thomas-Fermi potential with an average exchange of Slater type added, a quite satisfactory value was obtained for the equilibrium density of Al with estimated corrections for zero-point energy and electron correlation, namely 2.65 g/cm^3 to be compared with the experimental 2.71 g/cm^3. It was noted, however, that the results are sensitive to the particular choice of potential. Because of the free electron behaviour of Al at normal density and the fact that plane waves exactly satisfy the spherical boundary conditions used in ref. 1), relatively good results were anticipated for this case. Further certain approximations of "free electron character" were made in the expression for the total pressure. In the case of Al such simplifications should lead to negligible errors. Consequently the application of the method to Al does not represent a very critical test of the method. The transition elements or the rare earths with their rather complex electronic structure provide a better proving-ground for determining the possibilities of the spherical cellular method. In this report we present results for Fe, and we will also include the results of calculations on Al and Fe with an approximate self-consistent potential. Our choice was fortunate, because recently Gandel'man[4] has published very similar calculations for these elements, and we can thus study the effects of various approximations, in particular the difference between Gandel'man's Hartree scheme and our Hartree-Fock-Slater approach.

The choice of Fe as a test case has many advantages. Firstly there are quite a few experimental results available such as the pressure-volume relation from both static[5a,b] and dynamic[6] experiments, and Mössbauer measurements[7] at high static pressures. Secondly, there are a fairly large number of theoretical investigations of the properties and electronic structure of Fe. These are in some cases based on rather elaborate methods and it is possible to make some detailed comparisons. The great interest in Fe is naturally caused by its magnetic properties and, from a calculational as well as conceptual point of view, by the effects and properties of the 3d-electrons. At least at normal densities, the 3d-electrons can neither be described as tightly bound nor as free. As one goes from the bottom to the top of the 3d-band, a smooth transition from a diffuse to a more contracted, atomic, nature of the 3d-wavefunction takes place[8]. The elaborate calculations of particular interest to us include the calculations by Stern[9], Henry[10], Gandel'man[3,4], and Gervat[11], which in different ways are concerned with

the bandstructure and the elastic properties of Fe at different degrees of compression. Stern has reported a calculation of the cohesive energy by means of a modified tight binding method. The total energy was calculated for three different values of the radius of the Wigner-Seitz sphere (R = 2.30, 2.66 and 3.10 a.u.), but no specific exchange or correlation effects were included. The total energy was minimized with respect to the radius of the sphere, R, and the number of electrons in the 4s-band. R comes out to be 2.66 a.u., which agrees excellently with experiments ($R_{exp} \simeq 2.67$ a.u.), as does the calculated compressibility. For the electronic configuration he further obtained $3d^7 4s$ (in his notations). Despite of all approximations Stern thus obtains very sensible results. Recently Ingalls[12] has used this tight binding method in a detailed analysis of the Fe^{57} isomer shift for different states of iron. Henry on the other hand used the method of orthogonalized plane waves (OPW). The total energy and the pressure were determined for five- to ten-fold compressions, which corresponds to such extreme pressures as hundreds of megabars. This is in a region where the statistical theories of the atom should give fairly reliable results. We note, however, that Henry's PV-curve (see figure 11) shows no tendency to approach the statistical curve and we are therefore inclined to believe that some errors are present in his calculation. Gandel'man has also computed the zeroisotherm: His results cover a large pressure domain and his PV-curve nicely approaches the statistical curve in the high density region. Finally there is Gervat's calculation. By means of the augmented plane wave method the bands of Fe were obtained for R = 2.66 and 2.1 a.u. The potential was obtained from the Thomas-Fermi expression for the charge density. No estimates of the corresponding pressures were made. All the calculations mentioned refer to a hypothetical non-magnetic state of iron.

In the following section the formalism of the spherical cellular method is outlined, and the choice of the potential and an iterative procedure is described. In the third section we present some results for Al and Fe, such as the bandstructure, the pressure-volume relation and some electronic properties. These results are compared with experiments and similar or more elaborate calculations, and from these comparisons we attempt to evaluate the accuracy and characteristics of the spherical cellular method and the approximations we have made.

2. Description of the model and the calculational procedures used.

The model can be characterized as a spherical version of the cellular method and is described in detail in reference 1). Within the assumed spherical atomic volume the crystal orbital, Ψ, is expanded in spherical harmonics.

$$\Psi = \sum_{l,m} B_{l,m} f_l(r)/r \cdot S_{l,m}(\theta,\varphi) , \qquad (1)$$

where the radial function, $f_l(r)$, satisfies the equation.

$$f_l''(r) + \left\{ -\frac{l(l+1)}{r^2} + 2\left[V_c(r) + V_x(r) + \epsilon\right]\right\} f_l = 0 . \qquad (2)$$

We have used the Slater approximation to the exchange potential, $V_x = 3\left\{\frac{3\rho(r)}{8\pi}\right\}^{1/3}$ where $\rho(r)$ is the electron distribution consistent with the Coulomb potential, V_c. As discussed below two different choices of V_c have been used. When the expansion (1) is introduced in modified Bloch conditions with wave-vector k applied to the sphere of radius R, one obtains, after multiplying with $S_{LM}(\theta\varphi)$ and integrating over the angles the following system of equations: $(L=0,1,2..L_{MAX})$

$$\begin{cases} \sum_{l=M}^{L_{MAX}} B_{lM} \cdot f_l(\epsilon;R)\, \alpha(l,L,M;kR)\left\{1-(-1)^{L}\right\} = 0 \\ \sum_{l=M}^{L_{MAX}} B_{lM} \left[R f_l'(\epsilon;R) - f_l(\epsilon;R)\right] \alpha(l,L,M;kR)\left\{1+(-1)^{L}\right\} = 0 \end{cases} \qquad (3)$$

where

$$\alpha(l,L,M;kR) = C_{norm} \int_{-1}^{+1} dx\, P_l^{|M|}(x)\, P_L^{|M|}(x)\, \exp(-ikRx) . \qquad (4)$$

$k \cdot R = \varkappa$ ranges from 0 to $(9\pi/2)^{1/3} \equiv \varkappa_0$. The resulting secular equation determines the orbital energies, ε, as function of k and R. These orbital energies give a bandstructure, in which each band is characterized by a definite M and the 'atomic' quantum numbers at k = 0, in which case the expansion (1) contains one term only.

We have performed calculations with two different choices of V_c. The first one, which was also used in reference 1), is the potential and charge distribution obtained from the Thomas-Fermi approximation applied to a finite spherical atom. The second choice is an attempt to obtain an essentially self-consistent potential. Gandel'man has also used a self-consistent potential, but he does not describe precisely in what sense he has achieved self-consistency. There are many different ways to do this approximately and we have used the following procedure. For k = 0 and a given potential,

the equation system determines an eigenvalue spectrum, in which each eigenvalue, the orbital energy ϵ, is characterized by a definite l and is degenerate with respect to M, $M \leq l$. In this spectrum there are two classes of solutions: One has $f_l(R) = 0$, which we will denote by a F and the other has $(r \cdot f_l'(r) - f_l(r))_{r=R} = 0$, denoted G. For a core state the F and G solutions are identical, and by counting the nodes in the radial function, f, the proper principal quantum number, n, may be assigned. From these radial functions, usually of the G-type, we can construct a new spherical symmetric charge distribution and potential by choosing occupation numbers, $p(n_i l_i)$, such that $\Sigma\, p(n_i l_i) = z$, the nuclear charge. For a given set of occupation numbers we then use an iteration procedure to obtain a restricted self-consistency, i.e. the eigenvalue spectrum does not change within a chosen numerical accuracy upon further iteration. In order to have a stable iteration procedure we use a suitable linear combination of the potential used to determine the radial functions and the potential derived from these functions: When starting from a Thomas-Fermi potential, 6 iterations are usually required, but this number can be reduced if a potential for similar occupation numbers and/or sphere radius is available.

With the potential constructed in the way described above, we proceed to solve the equations (2) and (3), and thus obtain a new set of k-dependent ϵ-values. This bandstructure is not consistent with the potential because, when constructing the potential, we have not used the expansion (1) and we have not chosen the occupation numbers from the resulting bandstructure and density-of-states. The calculation could, of course, be made self-consistent in this general way, but the computations would be too time-consuming and in general we do not expect to obtain any significant changes. In some test cases, however, we have attempted to determine self-consistent occupation numbers in the following way: When the bandstructure and the occupied states are determined, we analyze the crystal orbitals in l-components. This gives a distribution of the z electrons over the different l-values. This distribution is used to choose new occupation numbers, $p(n_i l_i)$, only considering the lowest l-values, say up to 2 or 3. We then proceed to iterate a new potential with these new p's, calculate the bandstructure and the occupied states and finally compare the l-analysis of the new solution with the chosen occupation numbers. Even this simplified procedure is quite time-consuming, and since the model itself at the most can give a semi-quantitive picture of the behaviour of compressed matter, we have not attempted to fulfill the self-consistency requirement more accurately.

The formulas used to compute the pressure have been derived elsewhere[1,3,13]. In the Hartree-Fock case the expression is:

$$P = P_{cell} + P_x + P_c \tag{5}(a)$$

$$P_{cell} = \frac{1}{S}\int_S dS \left\{ \frac{\partial^2}{\partial \vec{r}\,\partial \vec{r}'} - \frac{\partial^2}{\partial \vec{r}^{\,2}} \right\} \gamma(r'1)\Big|_{\substack{\vec{r}\in S \\ r'\to 1}} \tag{b}$$

$$P_x = -\frac{1}{3v}\sum_{R_g\neq 0}\int_v d\vec{r}_1 \int_v d\vec{r}_2 \frac{\gamma(12)\gamma(21)}{|\vec{r}_1 - \vec{r}_2 - \vec{R}_g|} \approx -\frac{1}{3} v^{-4/3}\mu(q) \tag{c}$$

$$P_c = \frac{1}{3v}\sum_{R_g\neq 0}\left[\frac{Z^2}{2|\vec{R}_g|} - 2Z\int_v d\vec{r}_1 \frac{\gamma(11)}{|\vec{r}_1 - \vec{R}_g|} + 2\int_v d\vec{r}_1 \int_v d\vec{r}_2 \frac{\gamma(11)\gamma(22)}{\{\vec{r}_1 - \vec{r}_2 - \vec{R}_g\}} \right] \tag{d}$$

$$\approx \frac{1}{3} q^2 v^{-4/3} \lambda$$

where v and S is the volume and surface, respectively, of the Wigner-Seitz cell.

$\vec{R}_g$ = a lattice-vector.

$\vec{n}$ = the outward normal unit vector.

γ = first order density matrix (spin-free).

The approximations for P_x and P_c are based on the assumption that we have a uniform electron density equal to q/v. We obtain q from the calculated electron density at the surface of the cell. For increasing q, $\mu(q)$ increases from 0 to an asymptotic form, $\mu(q) \sim q$. In eq. (5d) λ is a small constant depending on the lattice structure. The formulas are easily simplified for a spherical atomic cell. The calculation of P_{cell} is quite straightforward, but a proper calculation of P_c and P_x which require multi-dimensional integrations, is far from trivial. The approximation with a uniform electron-density is reasonable for a free-electron like substance with small ion cores. One would thus expect accurate results for Al, but for Fe with its 3d-band, the approximation may not be reliable. This uncertainty must be remembered when discussing the computed pressures.

Gandel'man[4] has also used an electron-gas approximation when computing the exchange part of the pressure. There are, however, two deviations from our treatment. In the general formula for P_x, Gandel'man has an expression equivalent with eq. (5c), but in the approximation to it, he does not exclude $R_g = 0$. The other deviation is connected with the choice of the electron density, $\frac{q}{v}$, to be used in the electron gas approximation. For an electron

gas $P_x = -\frac{1}{4}(\frac{3}{\pi})^{1/3}(\frac{q}{v})^{4/3} = -\frac{1}{3\pi^3}E_F^2$ where E_F = Fermi energy = $\frac{1}{2}(3\pi^2)^{2/3}(\frac{q}{v})^{2/3}$.

As mentioned above we have chosen to obtain q from the calculated electron density at the surface of the cell, whereas Gandel'man prefers to use the Fermi energy. (More specifically, the Fermi energy relative to the potential at r = R.) Using the free electron formulas given above we can compute a q corresponding to Gandel'man's choice. For any deviation from a free-electron spectrum, the two q's will not be identical, but it is impossible to decide which q gives the best approximation. It is evident from the results reported in Table 1, that the differences can be quite large.

Table 1. Comparison of different choices of the electron density (q/v) to be used in the calculation of the pressure (eq. 5c and 5d).

	Al			Fe		
R	q	q_1	q_2	q	q_1	q_2
3.0	2.503	2.630	$E_2 < 0$			
2.8	2.715	2.752	$E_2 < 0$	1.579	0.442	1.531
2.6				1.854	0.453	1.137
2.4	3.136	2.970	0.171	2.153	0.424	0.766
2.2	3.350	2.846	0.510	2.434	0.384	0.413
2.1	3.514	3.055	0.790			
1.9	3.872	2.858	1.247			
1.8	3.939	2.603	1.421			

q is obtained from the calculated electron density at r = R.
$q_i = \frac{4}{9\pi}R^3(E_i(R_y))^{3/2}$; E_1 and E_2 are the Fermi energies relative to the bottom of the conduction band and $V_c(r = R)$ respectively.

The numerical calculations have been performed on an IBM 7090-computer. The solution of eq. (2) is obtained by a standard Runge-Kutta method in which the integration steps are automatically adjusted to give a specified accuracy. For each case the integration points are determined at the first integration and then fixed. The integration is carried outwards, and when iterating the potential, the boundary conditions for the core states are satisfied at a radius R' smaller than R, where R' is chosen so that the correct $f_1(r)$ is essentially zero for $r > R'$. The ε-values for which the secular determinant is zero are determined in the following way. For three chosen ε-s we obtain the value of f_1 and f_1' at r = R by numerical integration and then the value of the secular determinant (Gauss elimination). Since $f_1(R)$ and $f_1'(R)$ are fairly smooth functions of ε, we use values interpolated from the ones already obtained numerically until the solution is located in a small ε-interval. We then perform numerical integrations to obtain accurate values of f_1 and f_1' in this small ε-interval, and these are used to determine the final ε and the expansion coefficients B in eq. (1).

3. Results and discussion*.

a) Electronic energy levels and bandstructure.

Al: In figure 1. we present the energy bands obtained from the iterated potential in which the configuration $[Ne](3sG)^2(3pG)^1$ was used. The calculated bandstructure is very close to the one obtained[1] with a Thomas-Fermipotential with Slater exchange. At R = 3.0, which corresponds to the normal density of Al, the bandstructure is in fact essentially identical to that of the free-electron limit which was studied in ref. 14. Upon compression the character of the bandstructure changes to one that is not free-electron-like, and this behaviour is found both with the Thomas-Fermi and the iterated potential. A mechanism for this change has been suggested[14] and can briefly be described in the following way. The effective potential acting on an electron consists of three parts: A screened Coulomb potential, a centrifugal term $(l(l+1)/r^2)$ and a l-dependent repulsive potential, which arises from the orthogonality condition with respect to the core-states. The repulsive potential will only be effective inside the ion core and for l-values present in the ion-core electron configuration. In the case of Al the ion-core radius, R_c, is roughly 1 a.u. and the electron configuration is $[Ne] = [(1s)^2(2s)^2(2p)^6]$. At the normal density, i.e. $R \approx 3.0$, the potential is thus expected to be essentially constant in the major part of the atomic volume, leading to free-electron bands. When R approaches R_c, the potentials for the different l-values may become quite different and far from constant, because the different contributions to the effective potential will not have the same dependence on the atomic volume. At extreme compressions, $R << R_c$, one would again obtain a free-electron behaviour because the potential energy will be proportional to $1/R$ and thus a small perturbation compared with the kinetic energy which will be proportional to $1/R^2$. The change in the bandstructure which occurs upon compression is also reflected in the l-component analysis of the conduction-band wave functions which is presented in Table 2. This analysis suggests that at $R \approx 2$ (3.5-fold compression) a transfer of electrons from s- to d-character occurs for a relatively small change of the volume. Comparisons between the chosen configuration and the component analysis reported in Table 2 indicate that self-consistency in the sense discussed in section 2 is not achieved, but the second entry for $R \approx 3.0$ suggests that one would not expect any major changes if self-consistens solutions had been used.

---

* We will use the units: 1 length unit = Bohr radius $\approx$ 0.52917 Ångström
1 energy unit = 1 Rydberg $\approx$ 13.60 eV.

In the case of an electron gas the spherical cellular model gives the correct l-occupation numbers if the number of electrons per atom, n, is less than or equal to 2. When $n > 2$, the inappropriate boundary conditions in the spherical model apparently introduce considerable deviations. For $n = 3$, which is relevant to Al, the l-occupation numbers for the electron gas treated by the spherical model are essentially identical to the ones for Al at normal densities ($R \approx 3$). This agrees well with the description of Al as free-electron like. In Table 3 we have tabulated the electron energies calculated with the iterated potential. For each band the value for $k = 0$ has been given. For all R-values the Coulomb potential at the spherical boundary is negative but numerically small ($< 10^{-3}$). For increasing R the spectrum approaches the free-atom values obtained by Hermann and Skillman[15] using the same approximation for the exchange potential. The energy differences between the core-states (1s, 2s, 2p) are essentially independent of the volume for $R \geq 1.8$, but with decreasing R the binding energy decreases giving at $R = 1.8$ a shift of approximately 18 eV relative to the free atom. In most measurements, however, the relevant reference energy is the Fermi level, and e.g. the energy of the 1s-level relative to the Fermi level differs from the 1s-binding energy for the free atom at most by ~ 7 eV for the volumes investigated ($3.25 \geq R \geq 1.8$).

Fe: Due to the presence of the partially filled 3d-shell with its localized electrons the bandstructure for Fe will be quite different from the one for Al. In figure 2 we have given two representative examples using a potential iterated with the configuration $(4s)^{0.45}(4p)^{0.30}(3d)^{7.25}$. The relative position of the 4s- and 3d-band is apparently the determining factor for the qualitative behaviour of the bands and their widths. In figure 3a we have plotted the position of the 4s-band relative to the 3d-band for some R-values using three different potentials and in figure 3b the Fermi level relative to the lowest state in the bands is given. It is quite clear, that the Thomas-Fermi potential with Slater exchange is not a satisfactory potential because, at normal density ($R \approx 2.67$), it gives a 4s-band lying above the 3d-band. Both theoretical and experimental work show that the opposite is true. According to Gandel'man[3] the correct order of the 3d- and 4s-band is obtained at normal density with a Thomas-Fermi potential if no exchange corrections are added. This neglect would, however, give rather poor values for the least bound core-states, and the correct order obtained with a TF-potential is probably fortuitous. In Table 2 the component analysis of the wave functions for the occupied parts of the 3d-and 4s-band are reported. The results suggest that it is not particularly appropriate to describe the bandstructure as a free-

electron band superimposed on a pure d-band constructed from localized orbitals.

The calculated one-electron energies of some states are given in Table 4. The 3d-wave functions are sensitive to the potential which makes it difficult to obtain self-consistency. The results show, however, that with the iterated potentials used, the core-states are quite stable and only slightly dependent on the atomic volume. This is not the case for the Thomas-Fermi approximation to the Coulomb potential.

At normal density ($R \approx 2.67$) the width of the 3d-band is 0.20 Ry when an essentially self-consistent potential is used in the spherical cellular model. The width computed with other methods varies from 0.68 Ry (modified tight-binding, Stern[9]) to 0.12 Ry (OPW, Callaway[18]). According to Stern[9] the values suggested by the experimentalists show a similar variation. With increasing compression we find an increasing band-width, and at R=2.2 we obtain 0.47 Ry.

3b) The density-of-states, electronic specific heat and the electronic Grüneisen γ.

In the analysis of experimental shock adiabats Altshuler[6] has used the concept of an electronic Grüneisen γ. In the Mie-Grüneisen equation-of-state,

$$P_{thermal} = \frac{\gamma}{V} E_{thermal}, \tag{6}$$

γ contains contributions from the lattice (γ_L) as well as the electrons (γ_e). For a free-electron gas the Mie-Grüneisen form is exact and γ_e has the value 2/3 (non-relativistic) or 1/3 (relativistic). In semi-empirical work for a real solid one usually assumes some analytical form for γ_e (or some related quantity) containing parameters to be determined by fitting to an experimental shock adiabat. It can be shown that, at temperatures well below the degeneracy temperature of the electrons, γ_e is related to the thermal electron energy, $E = \frac{1}{2} \cdot \beta T^2$ by

$$\gamma_e = - \frac{\partial \log \beta}{\partial \log \delta} \tag{7}$$

where δ is the relative compression. β is determined by the density-of-states, $g(\epsilon)$, at the Fermi energy, ϵ_F, by the formula

$$\beta = \frac{1}{3} \pi^2 k_B^2 g(\epsilon_F), \quad k_B = \text{Boltzmann's constant.}$$

A knowledge of $g(\epsilon_F)$ as function of volume is thus sufficient to determine the physically interesting quantities β and γe and their volume dependence. If the temperature is not low, the calculations are slightly more complicated as discussed by Gandel'man[3,4].

The density-of-state is thus particularly interesting in the discussion of the thermal electronic properties of condensed matter but is also of importance in other connections such as optical properties. If the lattice symmetry of a crystal is properly taken into account, it is a tedious task to calculate the density-of-states even if one limits oneself to the Fermi energy. The reason is that in general the energy bands are required for many directions in k-space and that the Fermi surface is often quite complicated. In the spherical cellular model none of these complications will be present due to the spherical symmetry in k-space. It is, however, important to remember that the crudeness of our model may introduce artificial peculiarities having no counterpart in the properties of a real system.

The calculated density-of-states curves for Al are displayed in figure 4. At normal density (R = 3.0) the curve is almost identical to the one obtained in the free-electron limit of the spherical cellular model[14]. Comparing with the correct density-of-states for free electrons (the dashed curve in figure 4(i)), it is evident that there are strong local deviations in the form of peaks and gaps. These are introduced by the model, and it is therefore difficult to decide which, if any, of the changes occuring upon compression have a physical significance. As shown in figure 5, the volume dependence of $g(\epsilon_F)$ and γ_e are quite different from the simple behaviour which one most certainly would introduce in a semi-empirical approach. The strong peak in the $g(\epsilon_F)$-curve is obviously associated with the flattening of the 3d-band and the redistribution in k-space of the occupied states. In figure 5 the dashed curves correspond qualitatively to Gandel'man's results[4]. The general characteristics - the peak in $g(\epsilon_F)$ and oscillatory behaviour of γ_e - are the same in Gandel'man's Hartree calculation and our Hartree-Fock-Slater method. This agreement indicates that the results are not critically dependent on the choice of potential. With proper symmetry conditions on the wave functions, the interpretation in terms of an effective potential (given in section 3a above) is still valid, and one would thus conjecture that the results have at least a qualitative similarity with reality. The actual magnitudes as well as the number of oscillations are, however, doubtful.

In figure 6 we show the density-of-states for Fe at R = 2.6. The results are obtained with an iterated potential using the configuration $(4s)^{0.45}$ $(4p)^{0.30}$ $(3d)^{7.25}$. The discontinuities and strong peaks are again introduced by the model and are associated with the essentially k-independent part of the bands at large k (compare figure 2). If our calculated data are used to construct a histogram, as one usually does, the result is, indeed, more similar to the ones obtained by other methods such as APW, OPW, etc. In a sense the histogram would have been a more appropriate way of presenting the calculated density-of-states, because it conceals the strong local variations which are introduced by the spherical model and which would not be present if the lattice symmetry had been taken into account.

The density-of-states at the Fermi energy is calculated to be 30 per atom and Ry at normal density (R = 2.67). This is in fair agreement with the experimental value 28.7 obtained from the electronic specific heat, but this does not mean too much because of the following fact. The normal form of iron is ferromagnetic whereas in all our calculations we have tacitly assumed a paramagnetic state. The ferromagnetism arises from an unbalance in the number of spin-up (N_+) and spin-down (N_-) electrons. Effectively the potential acting on an electron is spin-dependent and in general the resulting energy difference between the two spin-states is not constant but depends on the wave-vector k[19]. If, however, we assume this energy difference, Δ, to be constant, we can easily simulate the ferromagnetic state by using the paramagnetic density-of-states (reduced by a factor two) for both spin-states. The values of $(N_+ - N_-)$ calculated in this way using different values of Δ are shown in figure 7. In order to obtain the 'correct' value, $(N_+ - N_-)$/atom = 2.2 at normal density, Δ has to be about 0.08 Ry which seems to be a reasonable average of Yamashita's results[19]. With $(N_+ - N_-)$/atom = 2.2 the calculated value of $g(\epsilon_F)$ for the ferromagnetic state is very large (10^3 to 10^4 states/atom Ry) in complete disagreement with the experimental value 28.7. This discrepancy is connected with the peak in the density-of-states curve which is caused by the maximum in $\epsilon(k)$ at large k of the 3d(M = 1) band. A summary of the calculated $g(\epsilon_F)$ is given in figure 8.

3c) The pressure-volume relation.

In principle there are at present theoretical methods (e.g. the APW-method) available which should give reliable predictions of the high-pressure properties of matter, but due to the extensive calculations required recourse is in most cases made to crude approximations such as various statistical models. The spherical cellular model provides an intermediate approach and it is therefore of particular interest to compute the pressure as a function of the volume.

As mentioned in the introduction the application to Al was promising when a Thomas-Fermi potential supplemented with Slater exchange was used. These satisfactory results are, however, not recovered when using a self-consistent potential of the type discussed in section 2. In figure 9 the results of various approximations are compared with a semi-empirical estimate[20] based on an extrapolation of shock-wave data. The increased compressibility which suddenly occurs at roughly a 3-fold compression is a consequence of the characteristic change in the bandstructure which is shown in figure 1. In the high-pressure region (1 Mbar - 100 Mbar) the two results with the self-consistent potential are similar, indicating that the effect of exchange in the potential is small in this case. At high compressions, the pressures obtained with the statistical models and the cellular models discussed in this report do not agree to the extent one had expected. We interpret this to mean that, in the case of Al, the statistical models are only satisfactory for pressures well above 100 Mbar (corresponding to a 10-fold compression). This pressure is considerably higher than what is commonly anticipated. Even at 100 Mbar the ion-core is only slightly influenced and at least a 30-fold compression is required before the wave functions of the electronic L-shell of Al are significantly affected by the boundary condition at the surface of the atomic cell.

If we turn our attention to small compressions the situation is considerably changed and becomes to a certain extent confusing. The results for Al and Fe reported in Table 5* clearly show that the reasonable values obtained in reference 1 were fortuitous. If at a given density exchange is included in the potential, the pressure will be lowered because the exchange potential is effectively attractive and, roughly speaking, will make the atom smaller.

---

* See next page.

Table 5. Results from various approximations for the calculated density, ρ_o, at P = 0 and the pressure, P, at the experimental ρ_o.

Al		Fe		Method
ρ_o g/cm^3	P kbar	ρ_o g/cm^3	P kbar	
2.71	0	7.87	0	Experiment
1.0	260	1.74	1750	Thomas-Fermi-Dirac[22]
3.33	-100	5.46	700	Thomas-Fermi with quantum corrections[21]
2.60	40	13.50	- 680	Spherical cellular model: TF-potential with Slater exchange
2.07	225	12.30	- 600	Spherical cellular model: TF-potential with Slater exchange excl. P_x
1.87	370	15.70	- 560	Spherical cellular model: Self-consistent potential with Slater exchange
?	585	12.30	- 330	Spherical cellular model: Self-consistent potential with Slater exchange excl. P_x
?	540	6.05	710	Spherical cellular model: Self-consistent potential Hartree model[4]
—	—	13.70	- 410	Spherical cellular model: Ferromagnetic. Self-consistent potential with Slater exchange
—	—	9.90	- 180	Spherical cellular model: Ferromagnetic. Self-consistent potential with Slater exchange excl. P_x

The results obtained for Fe, which are given in figures 10 and 11, and Table 5, also suggest that at normal density (R = 2.67, ρ = 7.87 g/cm^3) the inclusion of exchange in the potential has a large effect on the pressure both for the Thomas-Fermi and the self-consistent potential. By using a potential, which is somewhere between the Hartree and the Hartree-Fock-Slater potential, it seems to be possible to obtain accurate results for Fe whereas this is not the case for Al. The rather poor results obtained with the spherical cellular model in the low-pressure region are probably to a large extent connected with the fact that the density at zero-pressure is determined by a delicate balance of sometimes large, positive and negative contributions to the pressure. Our model does not take into account the effects of the lattice symmetry in a correct way and we have used a fairly crude approximation to the term P_x in equation 5. In particular, different choices of q, defined and discussed in section 2 (p. 8.), have a great influence on P_x for Fe but not for Al.

The calculations on Fe are performed for a paramagnetic state and the comparison with the experimental results relevant to a ferromagnetic state is therefore somewhat misleading. If our treatment of the ferromagnetic state discussed in section 3b can be trusted, there would be a substantial dif-

ference between the pressures of these two states (compare figure 10). At R = 2.67, corresponding to the normal density, 7.87 g/cm^3, the difference is approximately 200 kbar. Figure 10 shows that the choice of potential has a rather large influence on the pressure at small compressions, but as indicated in figure 11 this choice is not critical at extreme pressures.

3d) The isomer shift of the Mössbauer line in iron.

If a decaying Fe^{57}-nucleus is bound in a crystal, the emission of the 14.4 keV γ-quanta can occur without recoil of the parent nucleus (Mössbauer effect). The observed γ-energy is, however, not the same as the one determined by the bare, static nucleus but small shifts exist. These are due to electro-magnetic interactions between the nucleus and the surrounding electrons and to the vibrations of the nucleus. In particular, the electrostatic interaction between the nuclear charges and the electrons causes a shift, the isomer shift, which can be shown to be related to the electron density $\rho(0)$, at the nucleus by the formula[23)]

$$h\,\nu_{isomer} = K \cdot \rho(0) \tag{9}$$

The constant, K, depends on the properties of the nucleus. From measurements of the isomer shift in iron-compounds in which iron exists in different states of ionization, one has determined K by using the $\rho(0)$ calculated with Watson's[24)] wave functions for the appropriate ionized state. With K known, the isomer shift observed in Mössbauer experiments can thus give information on the electron density at the nucleus and the changes caused by e.g. different lattices and/or magnetic structures or by compression of the solid. As mentioned in the introduction, Ingalls[12)] has recently analyzed the experimental results by using the $\rho(0)$ obtained with Stern's[9)] wave functions. Qualitatively Ingalls obtains a consistent description, but the various experiments lead to some ambiguity in the correct value of K. It is evident that the $\rho(0)$ computed from the spherical cellular method cannot be used to give an accurate description of e.g. the effect of lattice symmetry or magnetic structures. We believe, however, that it can give some information on the validity of various approximations introduced in other calculations of $\rho(0)$.

In the experiments one measures the relative velocity, ε, between emitter and absorber necessary to produce resonance. With a common absorber, two different emitters would thus produce a shift, $\Delta\varepsilon$, in the velocity required, and for a pure isomer effect one obtains $\Delta\varepsilon = \alpha\Delta\rho(0)$ where $\alpha = \frac{\varepsilon}{E_\gamma} \cdot K$ using equation (9). Unless otherwise said, we will in the following use the value

$\alpha = -0.47$ (a u.)^{3}mm/s to obtain the experimental $\Delta\rho(0)$. The experimental shifts also contain a contribution from the nuclear vibrations, but, as shown by Benedek[23], in the experiments to be discussed, the vibrational contribution is small, and therefore it is reasonable to interpret the experimental shifts as an isomer effect.

In Table 6 we give the contribution to $\rho(0)$ from different electronic states for the free atom (ion) and the condensed state. For the finite atom the electron density at the nucleus is for the 1s-,2s-,and 3s-state systematically larger than for the free atom. It is difficult to believe that, in particular, the 1s- and 2s-state are really influenced by the finite volume. We suggest that the difference is due to the Slater approximation for the exchange potential, which was used for the finite volumes, whereas the values for the free atom and ions are obtained from proper Hartree-Fock calculations. The contributions from 1s and 2s are as expected essentially independent of the volume when the approximate self-consistent potential is used. This is not true for the Thomas-Fermi potential indicating that this potential is not reliable or that our approximate, analytical representation[1] of the Thomas-Fermi charge distribution contains systematic errors. It is clear, however, from the three separate calculations on the free atom with the configuration $(3d)^6(4s)^2$ that the electron density at the nucleus is quite sensitive to the accuracy of the wave functions. For the core states, in particular for 1s, the values given in Table 6 are for convenience given with higher numerical accuracy than the one which is significant. In our calculation the accuracy in the numerical integration of the radial wave functions should lead to 3 or 4 figures.

Watson's results for Fe^{2+} and Fe^{3+} give $\Delta\rho(0) = -1.90$, implying $\alpha = -0.47(au)^3$mm/s. The value of $\Delta\rho(0)$ contains the contributions +0.42, 0.00, and -2.32 from 1s, 2s, and 3s respectively. It is surprising and questionable that the contribution from 1s is so large and the value $\alpha = -0.47$ would therefore be uncertain.

Mössbauer experiments[7,23] on compressed iron in the body-centred cubic, ferromagnetic state give $(V\frac{\partial\epsilon}{\partial V})_{V=V_o} = (1.34 \pm 0.05)$ mm/s, which leads to $(V\frac{\partial\Delta\rho(0)}{\partial V})_{V=V_o} = -2.85(au)^{-3}$. From the densities calculated with the spherical cellular model applied to different volumes, we obtain $(V\frac{\partial\Delta\rho(0)}{\partial V})_{V=V_o} = 3.15$ from the 4s- and 3d-band, with -2.90 as the contribution from the 4s-band. These values are in reasonable agreement with experiment. As shown in Table 6 the density, $\rho(0)$, from the 3s electrons does change with the volume, and

when this effect is included we obtain $(V\frac{\partial \Delta\rho(0)}{\partial \Delta})_{V=V_o} \approx -6.0$, which is quite different from the "experimental" value. Ingalls[12] reports the value -4.9 ± 0.5 containing approximately 3 % from the 3s electrons to be compared with the 50 % contribution obtained in the spherical cellular model. The electron density at the nucleus of one 4s-electron is considerably larger in the solid than in the free atom. For the solid, our model and Ingalls' analysis give very similar results, 7.4 and 7.1 respectively. The value obtained by truncation and renormalization[26] of the 4s-wave function of the free atom is 8.4 (compare Table 6 column marked II). This suggests that there is a difference between the 4s-wave function in the free atom and the solid. In our model the density resulting from the 4s- and 3d-band is inversely proportional to the volume (see Table 6 column marked I), except at R = 2.2 where the relative position of the 3d- and 4s-band has changed. This dependence on the volume supports Benedek's method[27] of estimating $\frac{\partial \rho_{4s}(0)}{\partial V}$. It is, however, important to realize that, if only the 4s wave function is scaled one has to take nonorthogonality terms into account, and if instead all the wave functions are scaled the estimate of $\frac{\partial \rho(0)}{\partial V}$ would be completely erroneous. At R = 2.67 the calculated density is 3.3, which is close to the value 3.1, corresponding to one 4s-electron in the free atom. We may interpret this to mean that the number of 4s-electrons in the solid is 3.3/7.4 = 0.45, which is slightly larger than the value 0.41 obtained in the 1-component analysis reported in Table 2 but slightly less than the corresponding estimate using Ingalls' results[12], 3.8/7.1 = 0.54.

The experimental difference in $\rho(0)$ between the paramagnetic and the ferromagnetic state is quite small, $\sim +0.02$ at 1040° K[12]. Constructing the ferromagnetic state in the way described in section 3b above the spherical cellular model gives at R = 2.67 $\Delta\rho(0)_{\text{para-ferro}} = +0.03$ and $+0.02$ with $N_+ - N_-)/\text{atom} = 2.1$ and 2.3 respectively, and $\Delta\rho(0)$ increases upon compression. The agreement is satisfactory but most likely accidental considering all the drastic approximations involved.

It is gratifying to note that the spherical cellular model appears to be capable of predicting reasonable values of such a local property as the electron density at the nucleus. The qualitative result of our calculation is that it is important to take into account the changes occuring in the less tightly bound core states (3s in Fe), and that it is difficult to obtain a reliable picture of the behaviour of the wave functions in the solid from the ones in the free atom.

4. Concluding remarks.

The purpose of the study presented in this report has primarily been to test the spherical cellular model and its applicability to compressed states of matter. In the previous section the results for Al and Fe, two elements with quite different electronic structures, were presented and discussed. It appears to be rather difficult to make a definite statement about the validity of the model and the various approximations made. From a physical point of view the model describes in a qualitatively satisfactory way the electronic shell- and bandstructure, which is a fundamental characteristic of the electronic properties of matter. This is promising, because it is a basic defect of the statistical models that the shellstructure is not incorporated in a correct way. This shellstructure seems to be noticeable even at very large compressions but in this region the pressures calculated from the statistical models and the quantum-mechanical spherical cellular model do not differ much relative to the total pressure. The statistical model and the model discussed in this report fail to predict the correct density at zero-pressure. This is understandable because the zero-pressure is a result of a delicate balance between large positive and negative contributions to the total pressure. The spherical cellular model has, however, the advantage that the physics of it includes the feature - the electronic shellstructure -, which is responsible for the characteristic periodicity of many properties of matter when they are studied as function of the atomic number. The results presented in this report show, however, that the choice of potential is critical as it is in most quantum-mechanical calculations, and, in particular, it is important to treat the exchange effects in a proper way. We have also used fairly crude approximations when calculating the contribution to the pressure from the interactions between compressed atoms. It is therefore impossible to obtain a definite test of the basic assumption in the model, namely the replacement of the correct boundary conditions at the surface of cellular polyhedron with approximate boundary conditions at the surface of a spherical cell. Our general conclusion from the calculations is, however, that an 'atomic' approach, such as the spherical cellular model, includes the major effects of the electrons in compressed matter, and it seems to be worth-while to continue the study of the model.

(Table 1. See page 8.)

Table 2. Occupation numbers for different orbital angular momenta (l) present in the occupied part of the conduction bands in compressed Al and Fe.

	Atomic sphere radius R	Configuration chosen when iterating the potential which gives the bands used in the analysis to the right				l-component analysis of the occupied part of the conduction band					
						l = 0	l = 1	l = 2	l = 3	l = 4	7≥l≥5
Fe		4sG	4pG	3dG							
	2.8	0.45	0.30	7.25		0.405	0.235	7.290	0.048	0.015	0.007
	2.6	0.45	0.30	7.25		0.410	0.263	7.240	0.061	0.019	0.007
	2.6	0.65	0.00	7.35		0.426	0.281	7.202	0.063	0.020	0.008
	2.4	0.45	0.30	7.25		0.400	0.275	7.215	0.077	0.024	0.007
	2.2	0.45	0.30	7.25		0.360	0.259	7.242	0.097	0.030	0.012
Al		3sG	3pG	3dG							
	3.25	2.00	1.00	—		1.575	1.175	0.147	0.051	0.022	0.030
	3.0	2.00	1.00	—		1.493	1.233	0.169	0.065	0.028	0.012
	3.0	1.55	1.27	0.18		1.496	1.225	0.170	0.065	0.035	0.009
	2.4	2.00	1.00	—		1.326	1.291	0.223	0.106	0.042	0.012
	2.2	2.00	1.00	—		1.260	1.291	0.247	0.124	0.047	0.031
	2.1	2.00	1.00	—		1.114	1.351	0.347	0.128	0.041	0.019
	2.0	2.00	1.00	—		0.692	1.396	0.800	0.099	0.011	0.002
	1.9	2.00	1.00	—		0.634	1.335	0.940	0.084	0.006	0.001
	1.8	2.00	1.00	—		0.610	1.284	1.016	0.080	0.005	0.005
Electron gas; Exact. Number of electrons/atom = n					n						
					0.4	0.316	0.078	0.006	0.000	0.000	0.000
					1.0	0.653	0.304	0.040	0.003	0.000	0.000
					2.0	1.036	0.777	0.168	0.018	0.001	0.000
					3.0	1.296	1.275	0.370	0.054	0.005	0.000
					8.0	1.956	3.348	1.980	0.595	0.107	0.014
Electron gas; Spherical cellular model						Identical with the exact for n ≤ 2					
Number of electrons/atom					3.0	1.532	1.194	0.174	0.067	0.028	0.005
					8.0	1.758	4.387	1.000	0.650	0.178	0.027

Table 3. The electron energies of Al at different compressions.

The energies, in Ry, are given for the state k = 0 and, if nothing else is indicated, a potential iterated with the configuration $(3s)^{2.0}\ (3p)^{1.0}$

R	$-E_{1s}$	$-E_{1s}$ [a]	$-E_{2s}$	$-E_{2p}$	$-E_{3s}$	$-E_{3d}$	$-E_{Fermi}$
∞ [b]	113.66	113.30	8.715	5.947	0.7445	–	.3582 [e]
∞ [c]	117.003	116.583	9.821	6.4366	0.7868	–	.4199 [e]
∞ [d]	117.002	116.582	9.821	6.436	0.7867	–	.4201 [e]
3.25	113.6596	113.246	8.6821	5.9166	1.0555	0.1990	.4141
3.1	113.5031	113.157	8.5587	5.7911	1.0661	-0.0498	.3465
3.0	113.4432	113.142	8.5025	5.7347	1.0809	- .0806	.3011
3.0 [f]	113.4708	113.161	8.5237	5.7561	1.0892	- .0722	.3094
2.8	113.3022	113.118	8.3713	5.6028	1.1073	- .1577	.1846
2.4	112.9313	113.129	8.0295	5.2550	1.1237	- .3976	- .1975
2.2	112.7114	113.218	7.8260	5.0399	1.0866	- .5791	- .5069
2.1	112.5982	113.313	7.7199	4.9222	1.0438	- .6916	- .7147
2.0	112.4982	113.440	7.6202	4.8027	0.9779	- .8195	- .9420
1.9	112.3821	113.565	7.5169	4.6677	0.8718	- .9722	-1.1829
1.8	112.2809	113.718	7.4267	4.5252	0.7138	-1.1484	-1.4373

a) Relative to the Fermi level.

b) Reference 15

c) —— " —— 17

d) —— " —— 16

e) The value given is the energy of the 3p state.

f) Configuration $(3s)^{1.55}\ (3p)^{1.27}\ (3d)^{0.18}$

Table 4. The electron energies of Fe at different compressions.

The energies, in Ry, are given for the state k = 0.

R	$-E_{1s}$	$-E_{2s}$	$-E_{2p}$	$-E_{3s}$	$-E_{3p}$	$-E_{3d}$	$-E_{4s}$	$-E_{Fermi}$
∞ a)	515.81	60.957	53.084	7.2691	4.8912	0.9625	0.5451	–
∞ b)	522.803	63.930	54.885	8.3785	5.5210	1.2157	.5203	–
∞ c)	522.746	63.872	54.829	8.3394	5.4848	1.2942	.5166	–
2.8 d)	515.642	60.714	52.849	6.9491	4.5656	0.7683	0.8958	0.6234
2.6 d)	515.626	60.741	52.874	6.9398	4.5463	0.7968	0.9146	0.5935
2.6 e)	515.628	60.698	52.836	6.9003	4.5079	0.7650	0.8966	0.5581
2.4 d)	515.651	60.765	52.900	6.9141	4.4997	0.8241	0.8956	0.5345
2.2 d)	515.711	60.799	52.939	6.8804	4.4180	0.8579	0.8036	0.4389
2.8 f)	518.637	60.604	52.857	7.4515	5.0737	1.1045	0.8490	1.0126
2.6 f)	517.022	59.946	52.134	7.1056	4.7235	0.8639	0.7739	0.6911
2.4 f)	515.233	59.188	51.305	6.6932	4.2944	0.6066	0.6318	0.3035
2.2 f)	513.242	58.302	50.344	6.2058	3.7533	0.3274	0.3597	-0.1818

a) Reference 15

b) —— " —— 17

c) —— " —— 16

d) The configuration $(4s)^{0.45}\ (4p)^{0.30}\ (3d)^{7.25}$ is used when iterating the potential.

e) The configuration $(4s)^{0.65}\ (3d)^{7.35}$ is used when iterating the potential.

f) Thomas-Fermi potential.

(Table 5. See page 15.)

Table 6. Calculated values for the electron density, $\rho(0)$, at the nucleus in iron.

R	$\rho(0)$ 2 el. in 1s	2 el. in 2s	2 el. in 3s	1 el. in 4s $\cdot$ k = 0	4s- and 3d-band	I	II	Ref
∞	10775.6_7	991.11	136.28	3.165	–	–		a $3d^6 4s^2$
∞		989.80	135.73	3.112	–	–		b $3d^6 4s^2$
∞	10755.7_7	987.94	136.06	3.042	–	–	3.042	c $3d^6 4s^2$
∞	10756.0_6	987.91	135.05	–	–	–		d $(3d)^8$
∞	10755.9_8	987.75	135.33	–	–	–		d $(3d)^7 Fe^+$
∞	10755.7_3	987.59	136.55	–	–	–		d $(3d)^6 Fe^{2+}$
∞	10755.3_1	987.59	138.87	–	–	–		d $(3d)^5 Fe^{3+}$
2.8	10833.1_2	999.09	145.86	6.399	2.835	2.840	7.437	e solid
2.67	–	–	–	7.3_8	3.27	3.275	8.366	e solid
(2.67)	–	–	–	7.1	3.8	–	–	f solid
2.6	10832.5_2	999.07	146.42	8.070	3.547	(3.547)	8.974	e solid
2.4	10832.4_2	999.25	147.06	10.698	4.578	4.510	11.306	e solid
2.2	10832.5_2	999.64	147.80	15.002	5.062	5.855	15.048	e solid
2.8	10861.	997.5	145.5	6.997	–	–	–	g solid
2.2	10822.	983.0	138,9	15.909	–	–	–	g solid

I. $\left(\frac{2.6}{R}\right)^3$ x (density from the 4s- and 3d-band at R = 2.6); i.e. pure scaling.

II. $\Psi^2_{4s}(0) \times \left[\int_0^R \Psi^2_{4s} dr\right]^{-1}$ where Ψ_{4s} is Watson's[25] wave function for the free atom $((6d)^6(4s)^2)$. Compare Pollak[26].

a) C. Froese[17]

b) E. Clementi[16]

c) R.E. Watson[25]

d) R.E. Watson[24]

e) Present work. Configuration $(3d)^{7.25}(4p)^{0.30}(4s)^{0.45}$ used when iterating the potential.

f) Ingalls[12]

g) Present work. Potential from the Thomas-Fermi atom.

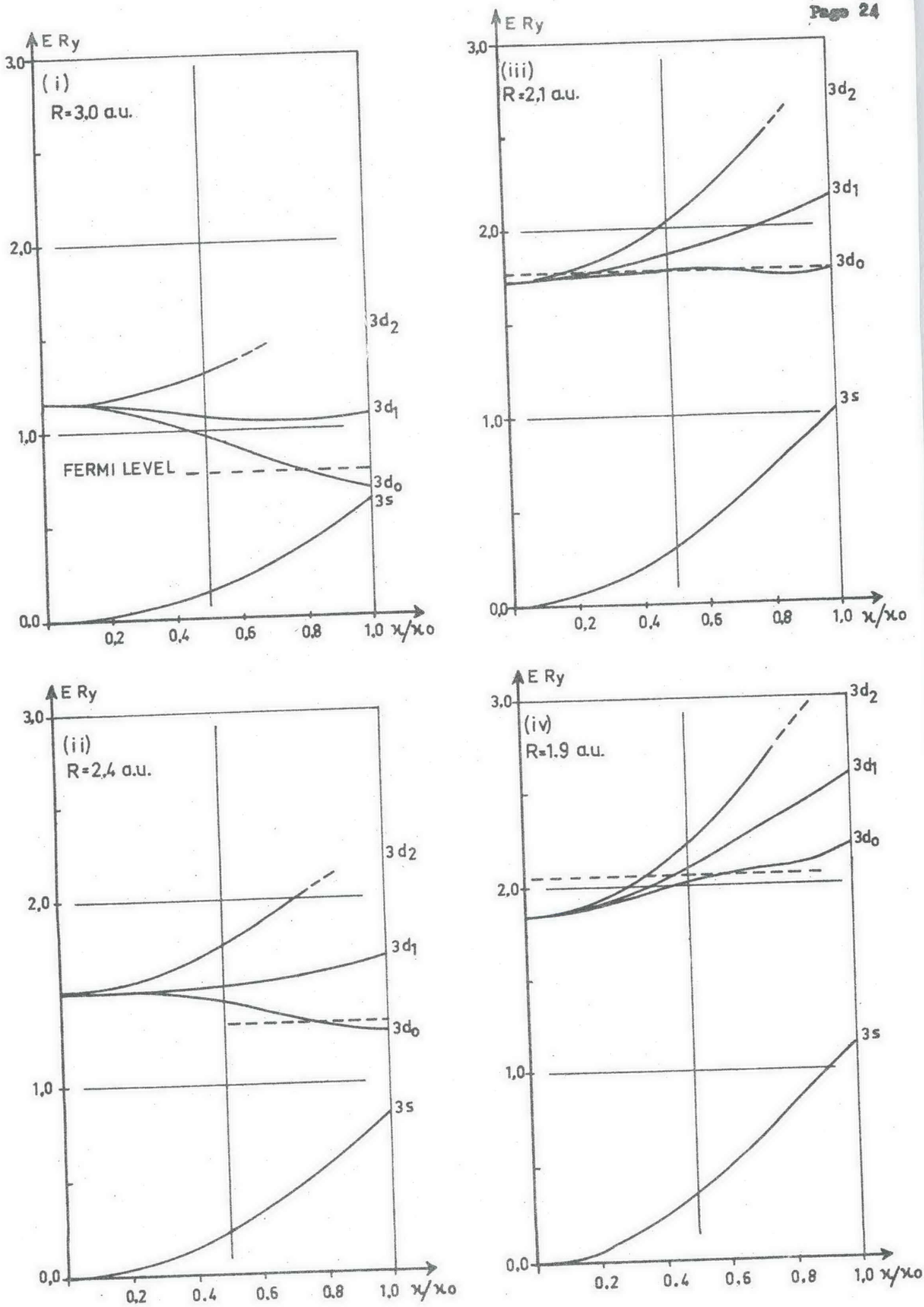

Figure 1: The energy bands for Al at different volumes.

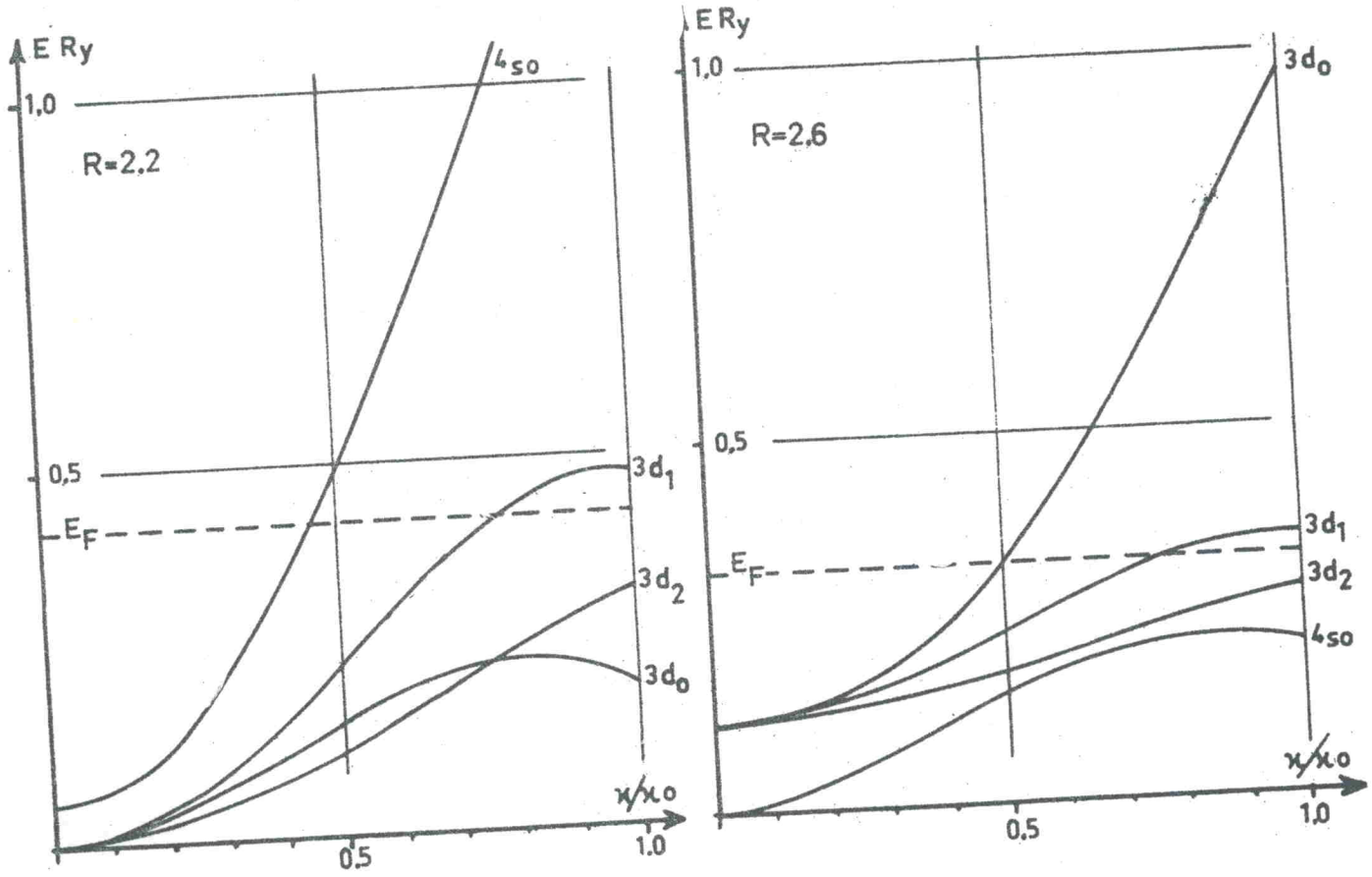

Figure 2: Energy bands for Fe. The potential used is approximately self-consistent.

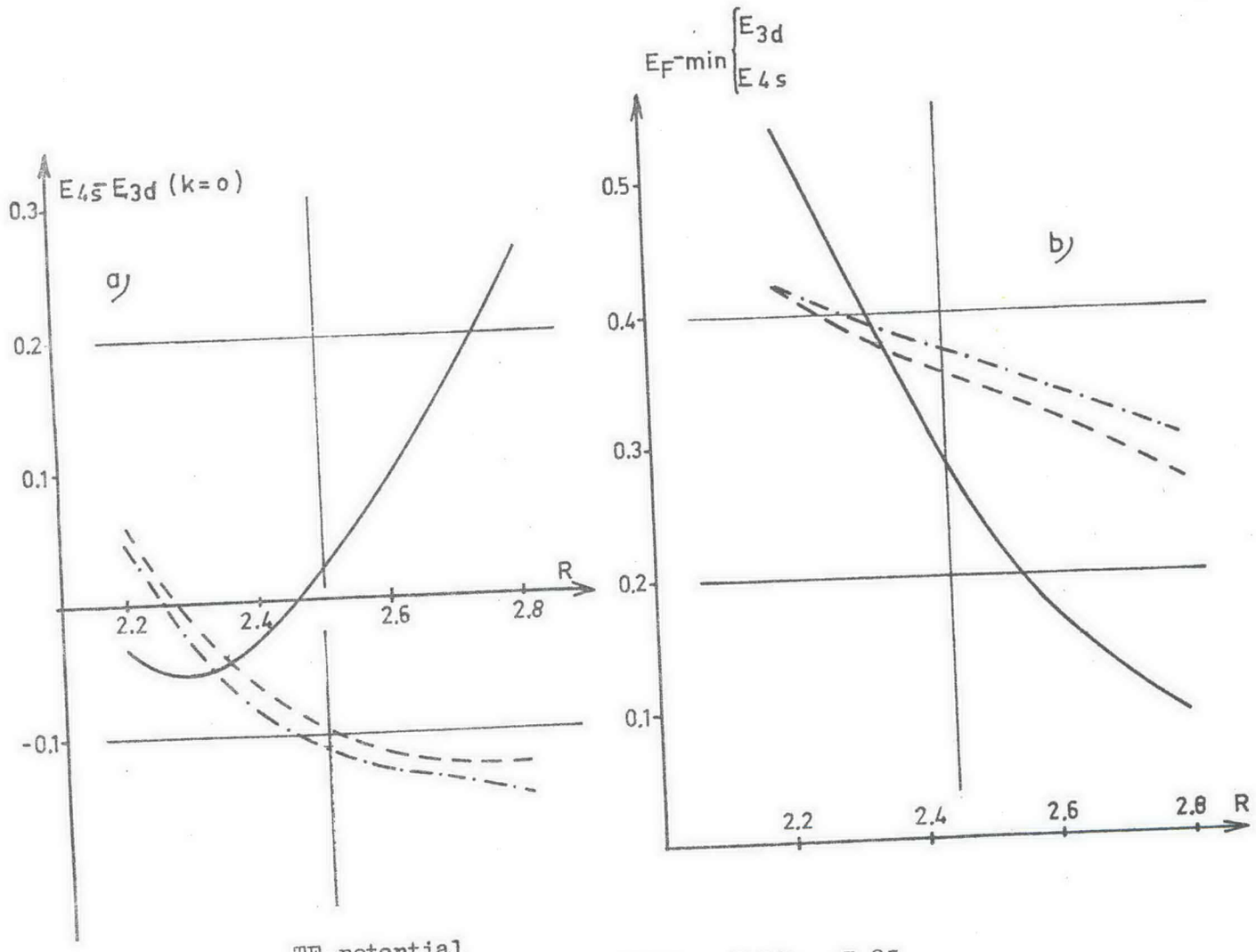

Figure 3: The relative position of the 4s- and 3d-bands in Fe at different compressions.

Figure 4: Density of states of Al for some different compressions according to the spherical model. The dashed curve in (i) indicates the exact free electron result. The notations s, d_0, d_1, and d_2 indicate to which bands the different parts of g(E) can be associated.

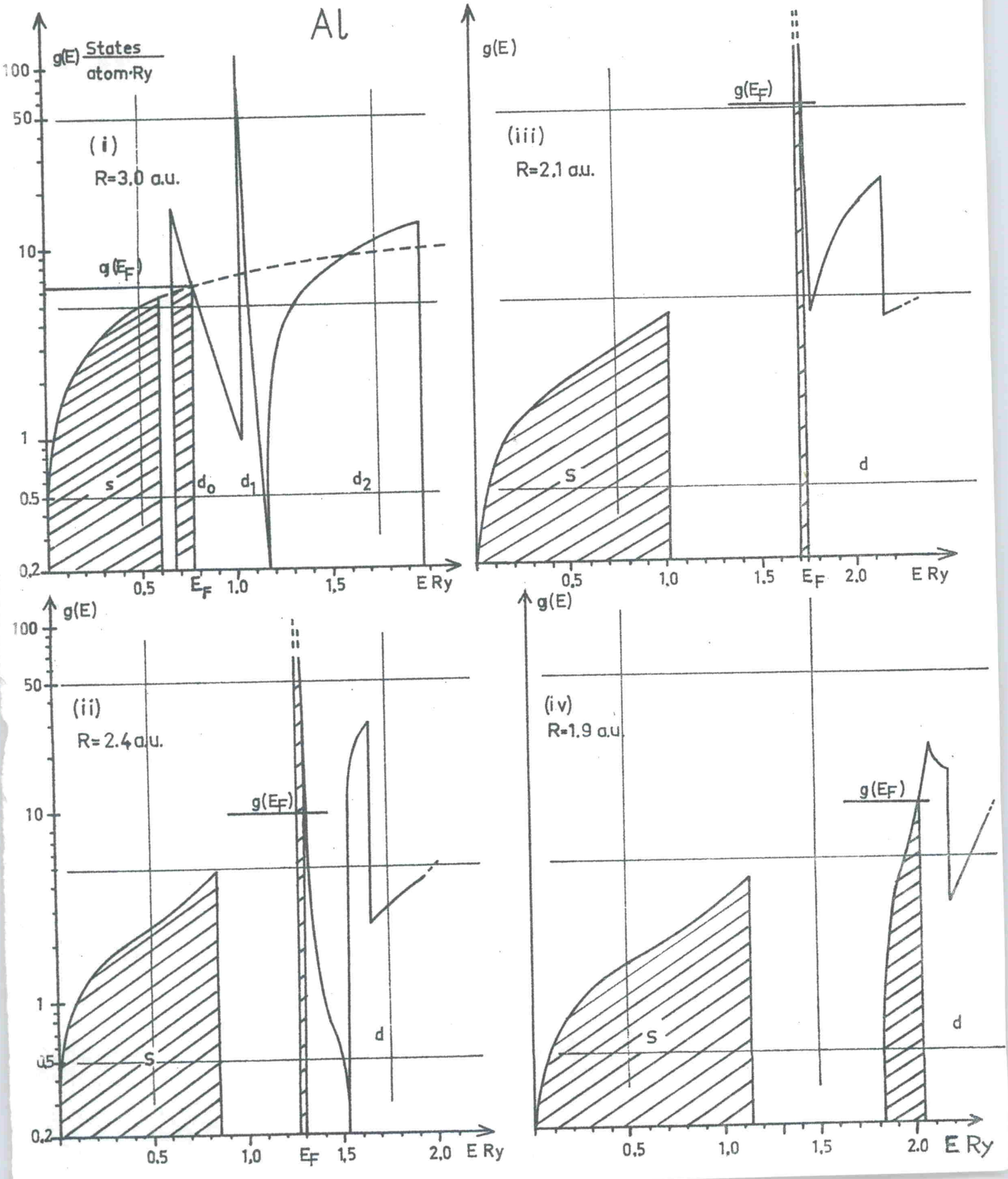

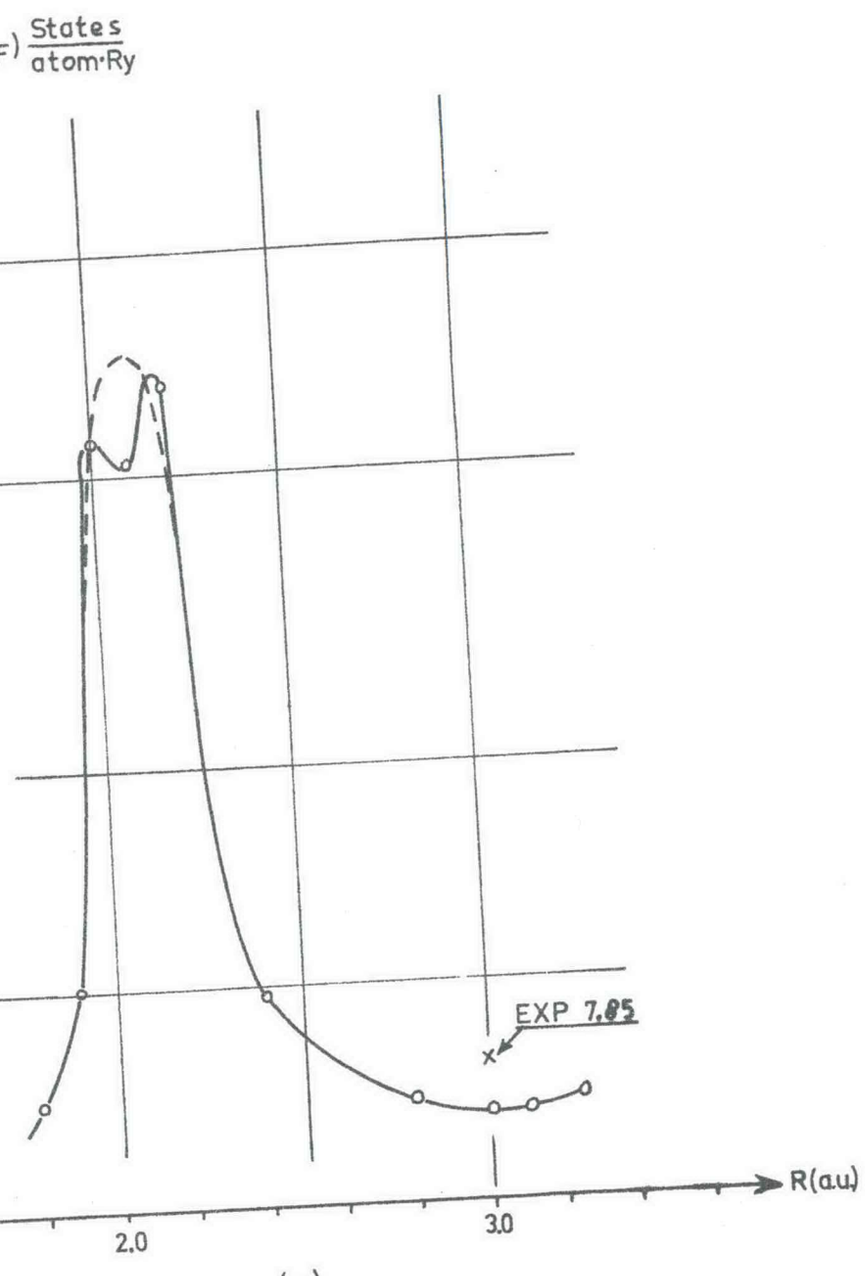

(a)

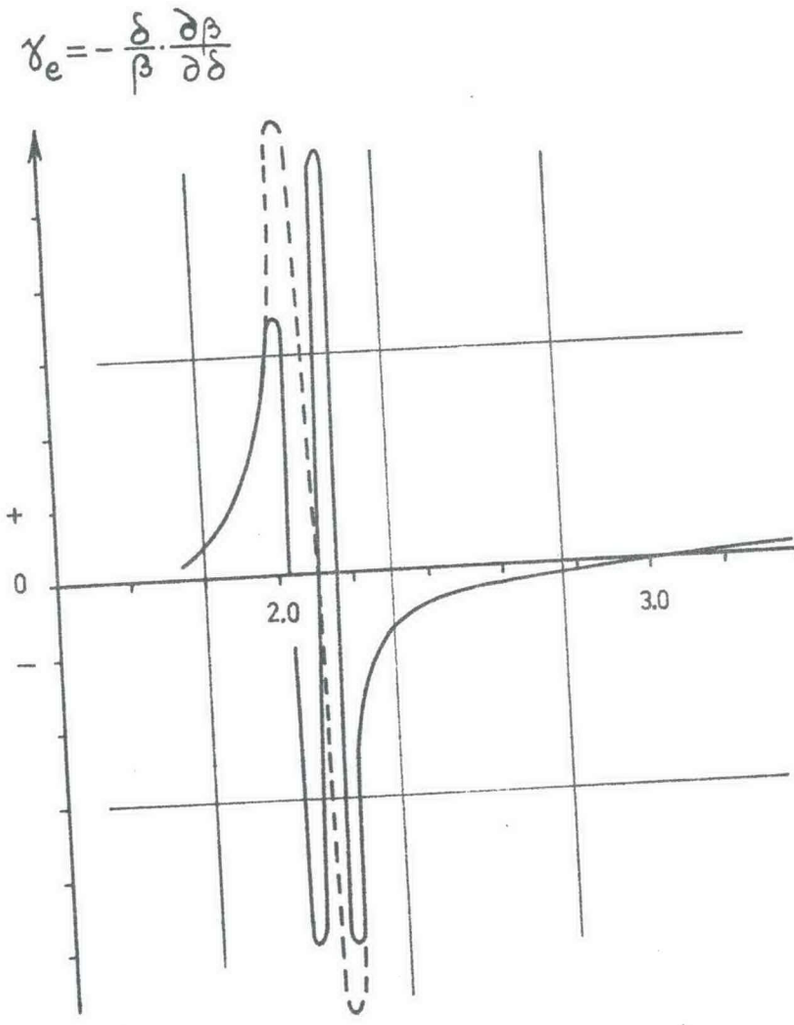

(b)

Figure 5: a) Variation for Al of the density of states at the Fermi surface, $g(E_F)$, as a function of the
the sphere. The calculated values are denoted by (O), and the experimental value at normal
(x). The dashed curve corresponds to Gandel'man's more smoothed results

b) Qualitative behaviour of the electronic Grüneisen constant. The curve is not drawn to scale
Note that a logarithmic scale is used in a) and a linear one in b).

Figure 6: Density of states for Fe at R = 2.6 a.u. according to the spherical model.

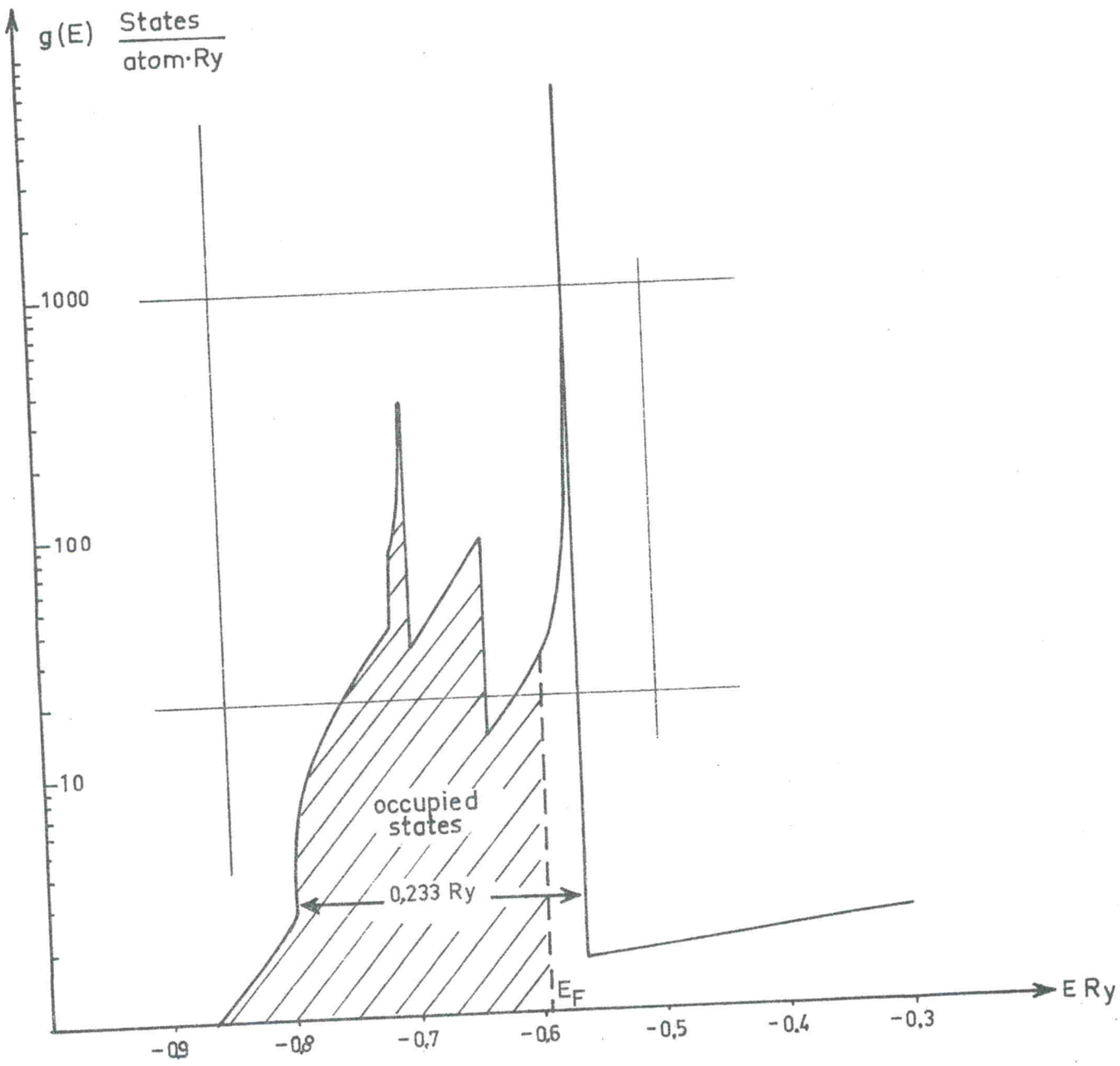

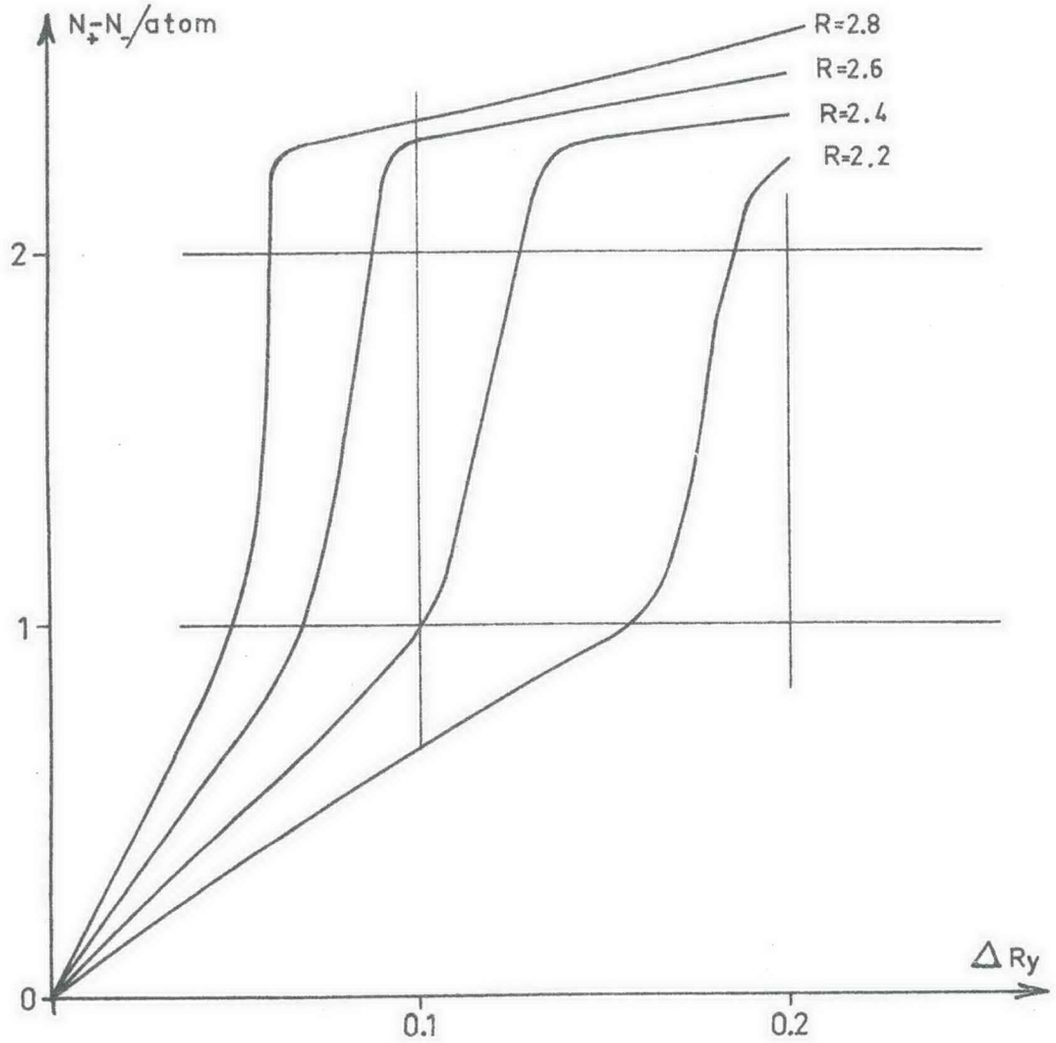

Figure 7: Variation of the number of "magnetic" electrons, $(N_+ - N_-)$/atom, in Fe as a function of the energy-separation, Δ, for different values of the radius of the sphere.

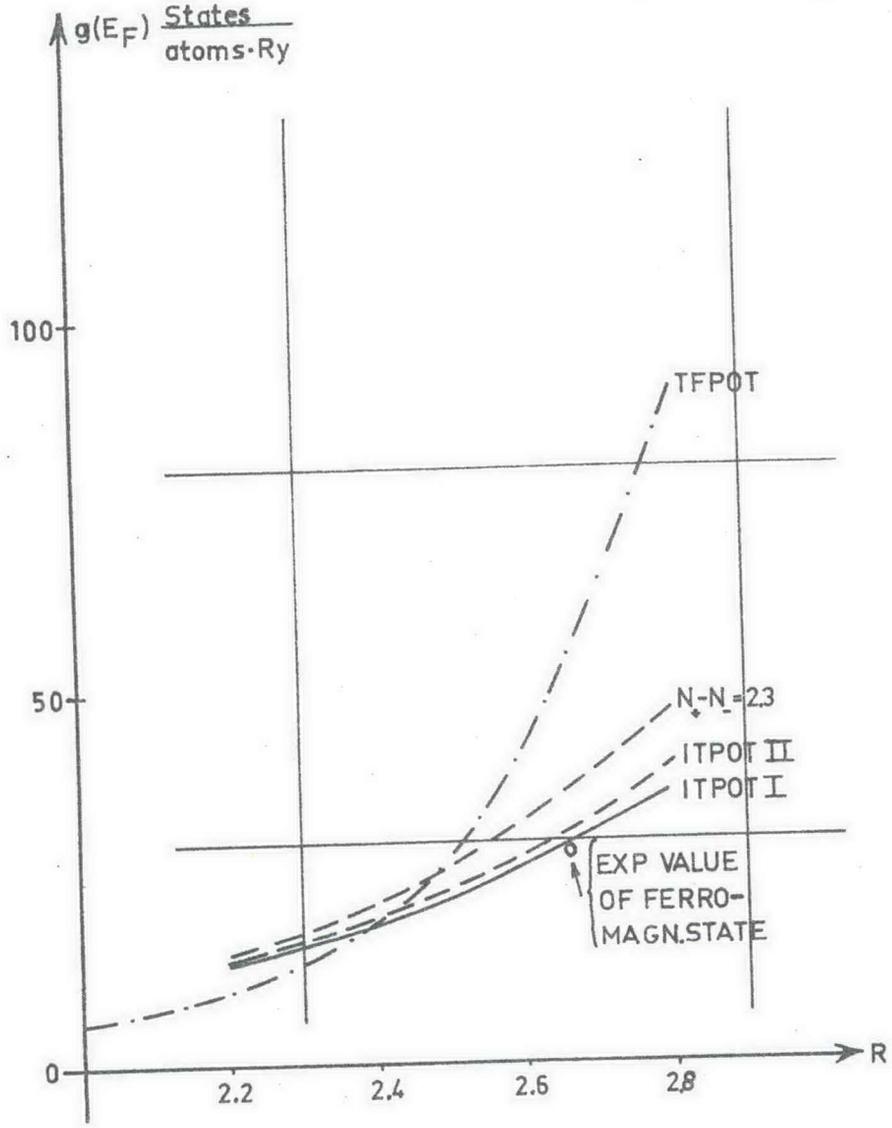

Figure 8: The density of states at the Fermi surface, $g(E_F)$, for Fe as a function of the radius of the sphere.

Figure 9: The total electronic pressure of Al at T = 0°K according to some different models:

a) Extrapolated semi-empirical relation from shock-wave data, (ref. 20)
b) Statistical model with quantum corrections (ref. 21)
c) Spherical model with Thomas-Fermi potential and Slater exchange (ref. 1)
d) Spherical model with an iterated potential as described in the text
e) Spherical model with iterated Hartree potential (ref. 4)

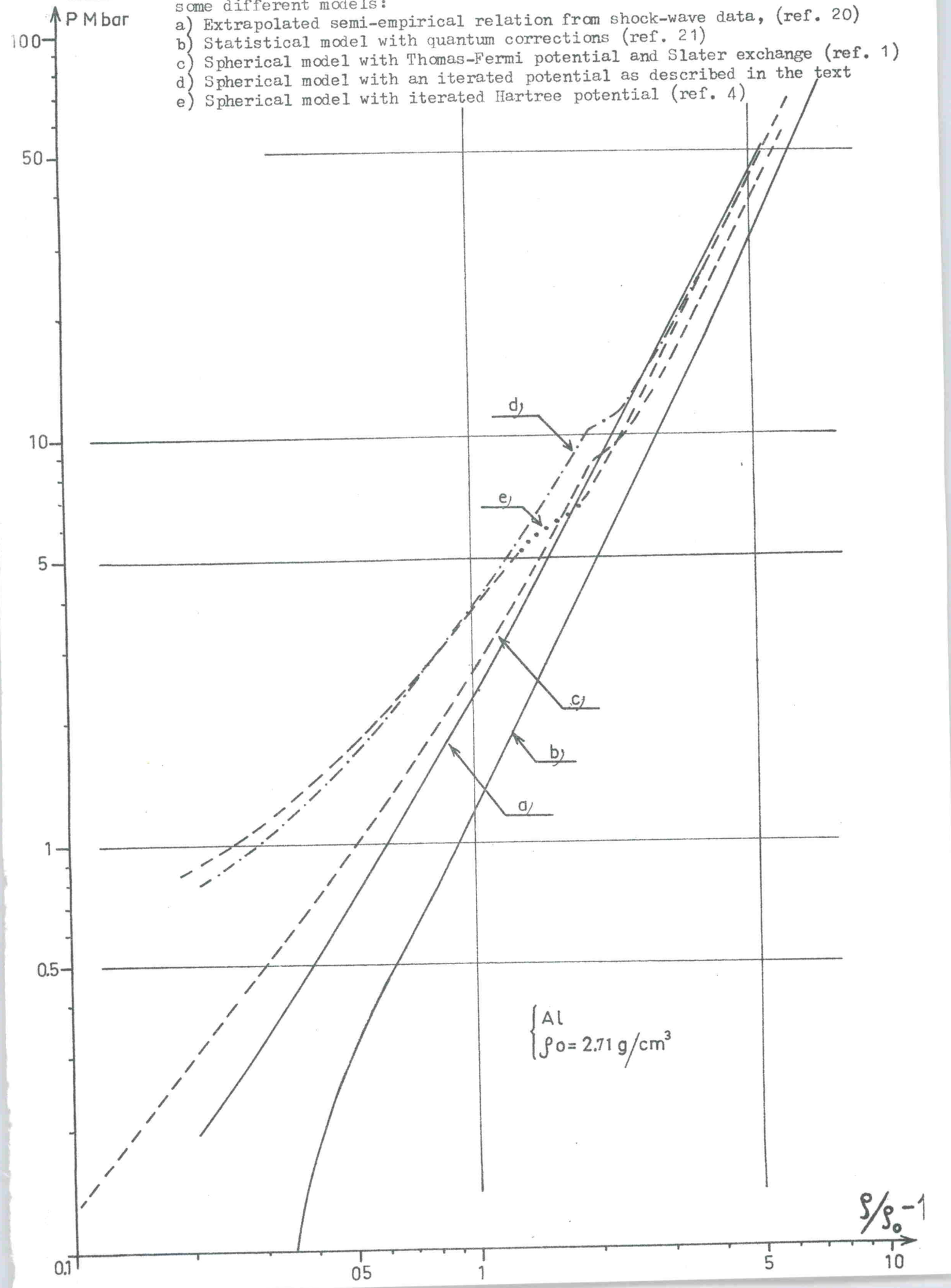

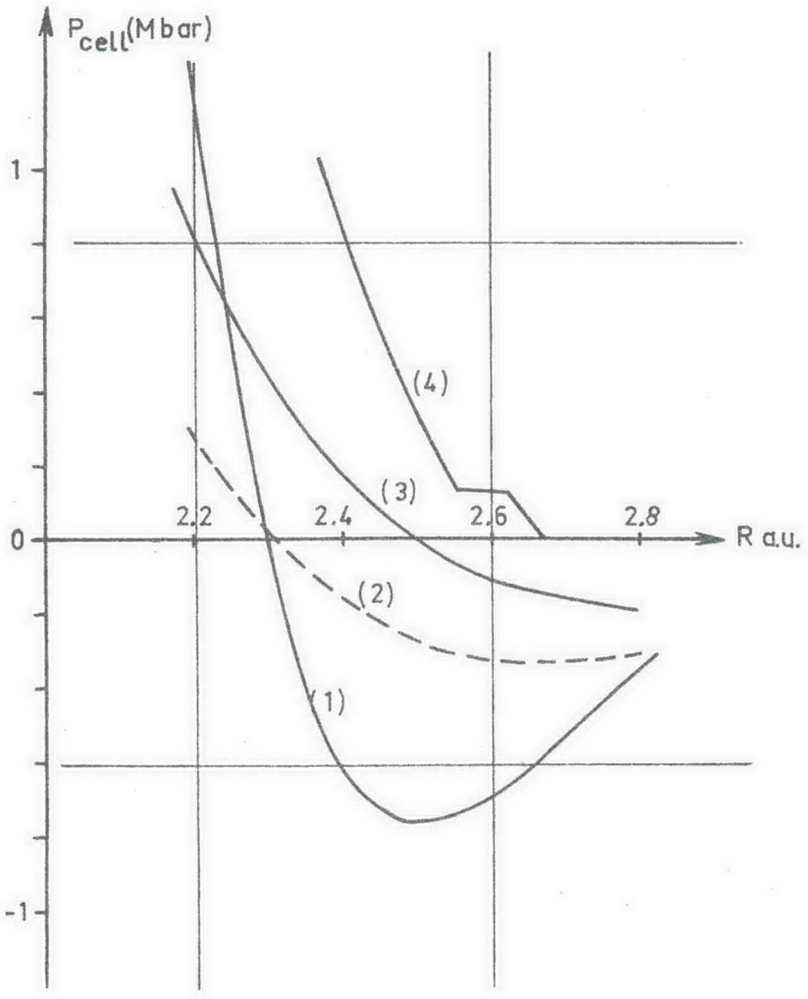

Figure 10: The calculated pressure in Fe at small compressions.

(1) P_{cell} with Thomas-Fermi potential with Slater exchange

(2) P_{cell} with self-consistent potential with Slater exchange

(3) Same as (2) but for the ferromagnetic state $(N_+ - N_-) \approx 2.2$/atom

(4) The experimental [5,6] total pressure.

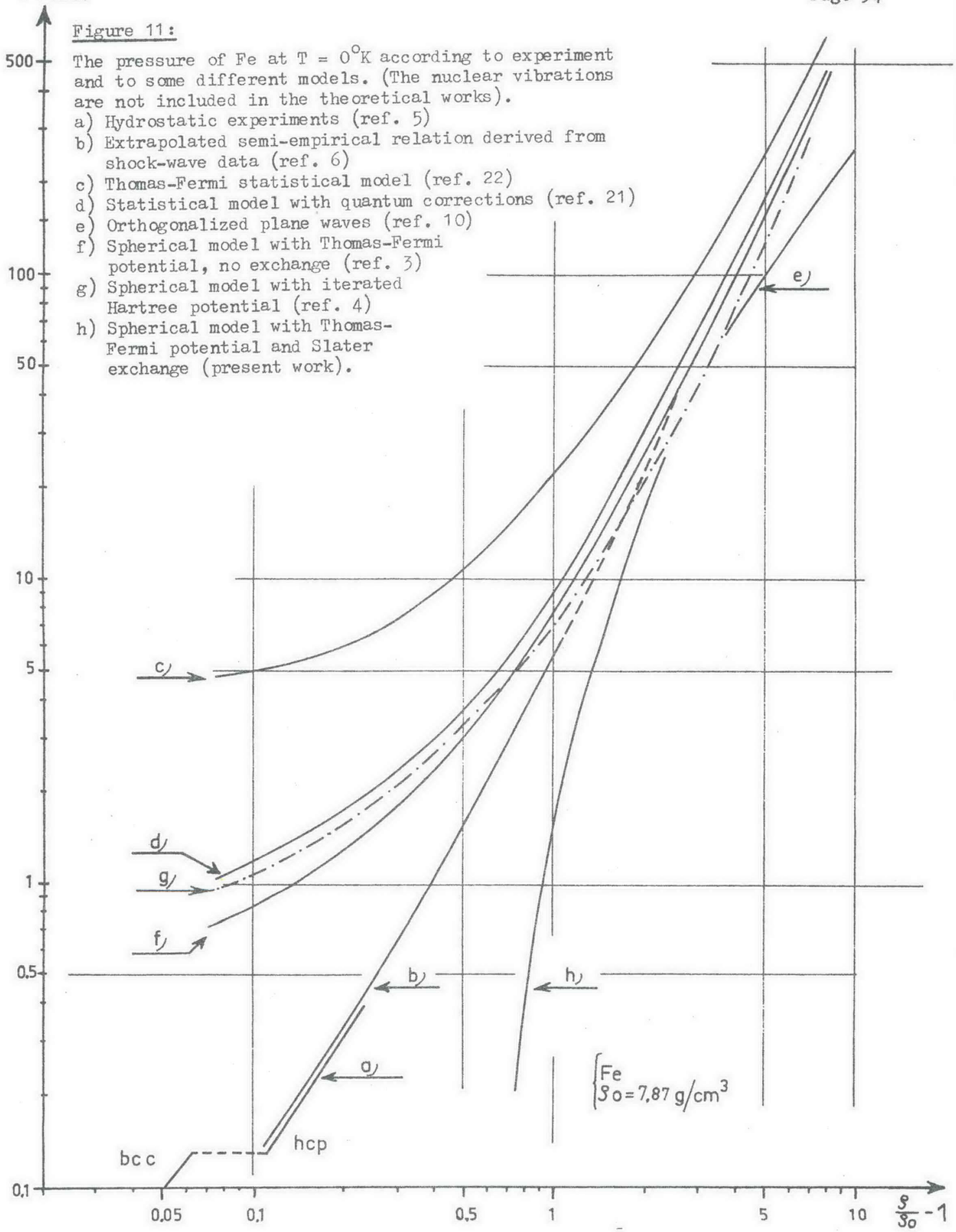

Figure 11:

The pressure of Fe at T = 0°K according to experiment and to some different models. (The nuclear vibrations are not included in the theoretical works).

a) Hydrostatic experiments (ref. 5)
b) Extrapolated semi-empirical relation derived from shock-wave data (ref. 6)
c) Thomas-Fermi statistical model (ref. 22)
d) Statistical model with quantum corrections (ref. 21)
e) Orthogonalized plane waves (ref. 10)
f) Spherical model with Thomas-Fermi potential, no exchange (ref. 3)
g) Spherical model with iterated Hartree potential (ref. 4)
h) Spherical model with Thomas-Fermi potential and Slater exchange (present work).

References.

1. Berggren and Fröman: Compressed atoms, FOA 4-report A 4444 July 1965.
2. H. Brooks, Nuovo Cimento (Suppl.) 7, 165 (1958).
3. G.M. Gandel'man, Soviet Phys. JETP 16, 94 (1963).
4. G.M. Gandel'man, Soviet Phys. JETP 24, 99 (1967).
5. a) Clendenen and Drickamer, J.Phys.Chem.Solids 25, 865 (1964)
   b) Mao, Bassett, and Takahashi, J.Appl.Phys. 38, 272 (1967).
6. L.V. Al'thsuler,Soviet Phys. Uspekhi 8, 52 (1965), and references given in this article.
7. Pipkorn et al., Phys.Rev. 135, A1604 (1964).
8. J.H. Wood, Phys.Rev. 117, 714 (1960); ibid. 126, 517 (1962).
9. F. Stern, Phys.Rev. 116, 1399 (1959).
10. J.F. Henry, Bull.Acad.Roy. Belgique Cl. Sci. 45, 553 (1959), ibid. 47, 344 (1961); J.Geophys.Research 67, 4843 (1962).
11. A. Gervat: "Quelques proprietés de la matière aux très hautes températures et fortes pressions (équation d'état, opacité)". Rapport CEA-R2603 (1965).
12. R. Ingalls, Phys.Rev. 155, 157 (1967).
13. N.A. Dimitriev, Soviet Phys. JETP 15, 539 (1962).
14. Berggren and Fröman: "On the free electron limit of the spherical cellular model". Preprint No 174 from the Quantum Chemistry Group, Uppsala University, Uppsala Sweden (June 1966).
15. Herman and Skillman: "Atomic structure calculations" (Prentice-Hall, Inc. 1963).
16. E. Clementi: "Tables of atomic functions". Supplement to IBM Journal of Res. and Development 9, 2 (1965).
17. C. Froese: "Hartree-Fock parameters for the atoms helium to radon". Unpublished report from Dept. of mathematics, Univ. of British Columbia, Vancouver (March 1966).
18. J. Callaway, Phys.Rev. 99, 500 (1955).
19. J. Yamashita et al. p. 497 in "Quantum theory of atoms, molecules, and the solid state". (Ed. P.O. Löwdin, Academic Press, 1966).

20. Berggren and Fröman: "Semiempirical equation-of-state for metals under high pressure". FOA 4-report A 4443 July 1965.

21. N.N. Kalitkin, Soviet Phys. JETP 11, 1106 (1960).

22. R. Latter: "Solutions of the Thomas-Fermi-Dirac statistical model of atoms". Report from RAND Corp. U.S.A. April 1964.

23. G.B. Benedek: "Magnetic resonance at high pressure". Interscience (1963). We have used this reference for general information on the Mössbauer effect.

24. R.E. Watson: "Iron series Hartree-Fock calculations". Technical Report No. 12, Solid-state and molecular theory group MIT (June 15, 1959).

25. R.E. Watson, Phys.Rev. 119, 1934 (1960).

26. H. Pollak, Physica status solidi 2, 417 (1962).

27. Reference 23, page 48.